Food Chemistry: X 27 (2025) 102369

Contents lists available at ScienceDirect

Food Chemistry: X

journal homepage: www.sciencedirect.com/journal/food-chemistry-x

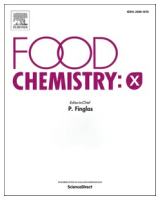

Epigallocatechin-3-gallate improved rheological properties of rice bran protein-soybean protein isolate conjugates emulsions by regulating interface protein conformation

Mengmeng Zhao, Xialing Wei, Xiaojuan Wu, Lizhong Lin, Wei Wu *

Faculty of Food Science and Engineering, Central South University of Forestry and Technology, Changsha, Hunan 410004, China

ARTICLE INFO

Keywords:
Rice bran protein
Epigallocatechin-3-gallate
Soybean protein isolate
Interface protein structure
Rheological properties

ABSTRACT

The effects of epigallocatechin-3-gallate (EGCG) on the conformation of interface-adsorbed protein (IAP) and interface-unadsorbed protein (IUAP) and rheological properties of rice bran protein-soybean protein isolate conjugates emulsions were investigated. The results showed that the viscosity, storage modulus, and loss modulus of conjugates emulsions initially increased, and subsequently declined as EGCG concentration increased (0 %–20 %), and reached the maximum value at an EGCG concentration of 10 %. Meanwhile, the absolute value of ζ-potential (−49.333 mV), average particle size (831.033 nm), and flexibility (0.052) of IAP reached the maximum at 10 % of EGCG. The absolute value of ζ-potential and surface hydrophobicity of IAP were higher than those of IUAP. Overall, moderate concentration of EGCG (10 %) enhanced the adsorption of highly flexible and highly surface-charged IAP at the oil-water interface and promoted the formation of a highly viscoelastic interfacial membrane, which improved the rheological properties of conjugates emulsions.

1. Introduction

Oil-in-water emulsions were homogeneous systems in which the oil phase, in the form of droplet, was scattered in the aqueous phase (Li et al., 2021). The emulsions were widely used in food, medicine, and cosmetics industries. As a food-grade emulsifier, protein was favored for its ability to adsorb at the oil-water (O/W) interface, which formed interfacial membranes that improved emulsion stability (Grasberger et al., 2023; Zolqadri et al., 2023). The construction of protein emulsions was usually the dynamic interfacial adsorption (via diffusion-permeation-rearrangement) process (Li et al., 2022; Lian et al., 2023). During this process, protein underwent structural changes, including exposure of hydrophobic groups, improvement in flexibility, and electrostatic repulsion (Kieserling et al., 2021; Lu, Xu and Zhao, 2022). These changes facilitated the interaction of interface proteins with neighboring interface proteins or oil phases to form highly viscoelastic interfacial film (Kim et al., 2020; Lu et al., 2019; Wu et al., 2024). Emulsions using animal protein as an emulsifier had been extensively studied (Bock et al., 2022; Kieserling et al., 2021). Vegetable protein was also an ideal emulsifier due to its amphiphilic and film-forming properties (Kristensen et al., 2021; Li et al., 2024). Vegetable protein was easier to extract, safer, more economical, and more sustainable than animal proteins (Hei et al., 2024; Tian et al., 2023). Therefore, the exploration of vegetable proteins stabilized emulsion was an important innovation subject with cost effectiveness and ecological efficiency (Hinderink et al., 2019). However, the complex structure (high content of hydrophobic amino acid residues and high molecular weight) and low solubility of vegetable protein resulted in weak viscoelasticity, which further reduced stability of vegetable protein-based emulsion (Drusch et al., 2021; Shao et al., 2024). Therefore, it was essential to enhance the stability of vegetable protein emulsions by modulating the conformation of vegetable protein at the O/W interface to improve the viscoelasticity of interfacial membrane.

Currently, studies on effect of interface protein structure on viscoelasticity of the emulsion interfacial film had focused on single protein (Grasberger et al., 2023; Li et al., 2021). Compared to the single protein, mixed proteins could simultaneously adsorb at the O/W interface to improve stability of emulsions due to the dense interfacial film through synergistic effect (Hinderink et al., 2019; Shen et al., 2023). Rice bran protein (RBP) was a premium emulsifier with amphipathicity. However, its emulsion stability was non-ideal (Zhao et al., 2024). Soybean protein isolate (SPI) with excellent emulsification stability was widely used in the food emulsion industry (Tan, Wu, Zhao, Li, & Wu, 2024). Previously, in our team, epigallocatechin-3-gallate (EGCG) covalently bound RBP

* Corresponding author.
E-mail address: foodwuwei@126.com (W. Wu).

https://doi.org/10.1016/j.fochx.2025.102369
Received 11 December 2024; Received in revised form 22 February 2025; Accepted 10 March 2025
Available online 12 March 2025

and SPI conjugates were prepared through alkaline pH-shifting (Wei et al., 2024). We found that EGCG could effectively enhance the stability of conjugates emulsion by modulating the spatial conformation of RBP-SPI compared to the stability of RBP emulsion and SPI emulsion alone. Noteworthy, when EGCG concentration was 10 %, the emulsion stability index of conjugates was even larger than that of the sum of RBP and SPI.

However, the effect of interface protein conformation on viscoelasticity of mixed vegetable protein emulsions had not been reported. The adsorption of mixed vegetable proteins at the O/W interface was critical as well as complex (Bock et al., 2022). It was necessary to reveal the potential mechanism by which EGCG regulated the interface protein conformation to influence the rheological properties of conjugates emulsions. Therefore, in this study, the rheological properties and interface protein conformation of RBP-EGCG-SPI conjugates emulsions were investigated. This study provided new perspectives on polyphenol to improve rheological properties and stability of mixed vegetable protein emulsions.

2. Materials and methods

2.1. Materials

Rice bran (Huang Hua Zhan) was purchased by Jinquan Rice Mill (Changsha, China). Defatted soybean meal was bought by Harbin Binxian Yuwang Plant Protein Co. Ltd. (Heilongjiang, China). EGCG (98 %) was bought at Shaanxi Jinkangtai Biotechnology Co. (Xi'an, China). 1-anilinonaphthalene-8-sulfonate (ANS) was acquired at Sigma-Aldrich Chemical Co. (USA).

2.2. Sample preparation

2.2.1. RBP and SPI preparation

The methodology of Wei et al. (2024) was referenced. The defatted rice bran powder was dissolved in deionized water at a ratio of 1:10 (*w/v*). The pH of the rice bran solution was adjusted to 9.0 with 2 mol/L NaOH solution, and stirred at 40 °C for 4 h. Then, the solution was centrifuged at 10,000 ×*g* at 4 °C for 20 min using a refrigerated centrifuge (Lynx 6000, Thermo Fisher Scientific, Germany), and the pH of the supernatant was adjusted to 4.0 with 2 mol/L HCl. After standing for 20 min, the solution was centrifuged at 10,000 ×*g* at 4 °C for 20 min to obtain precipitates. Then, the precipitates were diluted with 1:5 (*w/v*) distilled water, and the pH of the solution was adjusted to 7.0 with 2 mol/L NaOH. Finally, the solution was dialyzed with distilled water for 24 h, and the solution was freeze-dried using a freeze dryer (FD5-4 T, SIM, USA) to obtain RBP. The protein purity of RBP was 77.47 % (*w*/w, dry basis).

The low-denatured defatted soybean meal powder was mixed with deionized water (1,15, w/v), and the pH of the mixed solution was adjusted to 7.0 with 2 mol/L NaOH solution. Then, the solution was stirred for 1 h at 25 °C and centrifuged at 8000 ×*g* for 20 min. The pH of the supernatant was adjusted to 4.5 with 2 mol/L HCl solution, and allowed to stand for 20 min and then centrifuged (8000 ×*g*, 20 min). The precipitates were dispersed and washed three times with deionized water, and the pH of solution was adjusted to 7.0 with 2 mol/L NaOH solution to dialyze for 24 h. The dialyzed solution was freeze-dried to obtain SPI. The protein purity of SPI was 89.92 % (w/w, dry basis).

2.2.2. Preparation of RBP-EGCG-SPI conjugates

Based on the approach of Wei et al. (2024). Briefly, RBP and SPI were mixed (1,1, *w*/w) and dissolved to obtain a mixed proteins solution (10 mg/mL). EGCG was added to mixed proteins solution, the final concentrations (*w*/w) of EGCG in the mixed solution were 0 %, 5 %, 10 %, 15 %, and 20 %, respectively. The pH of mixed conjugates solution was adjusted to 12.0. The conjugates solution was reacted with stirring at 25 °C for 1 h. The pH of mixed conjugates solution was adjusted to 7.0. Then, conjugates dispersion was dialyzed (molecular weight cutoff of 8 kDa) for 24 h to remove small molecule impurities.

2.2.3. Construction of conjugates emulsions

The methodology of Wei et al. (2024) was referenced. The conjugates were combined with soybean oil (4,1, *v*/v), and subsequently high-pressure homogenized (D-6 L, pH.D. Technology LLC, USA) (80 MPa) three times after shearing (T18basic, IKA, UK) (10,000 rpm, 2 min) to obtain the conjugates emulsions.

2.3. The microstructure and rheological properties of conjugates emulsion

2.3.1. Appearance and microstructure

The prepared emulsion was loaded into a glass sample bottle and photographed to obtain the appearance of the emulsion.

Based on the approach of Li et al. (2021). Briefly, the microstructure of emulsions was examined using a biomicroscope (XDS-200C, Shanghai Caikang Optical Instrument Co.) with a 40× objective.

2.3.2. Viscosity and viscoelasticity

Based on the approach of Li et al. (2021). The viscosity of emulsions was determined under shear rates from 0.1 to 100 s^{-1} with 60 mm parallel plate at 25 °C using a rheometer (DHR-2 dynamic shear rheometer, TA, USA). The data was tested within a linear viscoelastic range of 1 % and a working gap of 500 μm. The data were fitted using the formula (Eq. (1))

$$\eta = kr^{n-1} \tag{1}$$

where the η, *k*, r, and n represented viscosity (Pa·s), shear rate (s^{-1}), consistency index (Pa·s^n), and flow index, respectively.

2.3.3. Viscoelasticity

Based on the approach of Li et al. (2021), with appropriate modification. The storage modulus (G') as well as loss modulus (G") of emulsions was determined under angular frequency from 0.1 to 100 rad/s. Other measured parameters were the same as the viscosity.

2.3.4. Creep-recovery

The methodology was referred to Lu et al. (2019), with slight modification. The experiment was conducted at a constant stress of 3 Pa. The creep phase lasted 300 s and recovery phase lasted 600 s.

2.4. Extraction of IAP and IUAP of conjugates emulsions

The methodology was referred to Li et al. (2021), with slight modification. Aqueous phase and the emulsions layer were separated after centrifugation of the freshly prepared emulsions. The separated emulsified layer was dispersed in phosphate buffer solution (10 mmol/L, pH 7.0), then centrifuged (18,000 ×*g*, 4 °C) for 30 min and washed twice. The aqueous phase was freeze-dried after being filtered by filters (0.45 μm) to obtain IUAP. The protein content of IUAP was determined by Bradford's method using bovine serum protein as a standard. The emulsions layer was combined with acetone (1:20, *v/w*) and centrifuged, the step was repeated five times. The collected protein was combined and dissolved in distilled water to get IAP after freeze-dried. The protein content of IAP (Γ) was calculated according to (Eq. (2)).

$$\Gamma = V_C\,(C_{IN}–C_{SE})/SV_O \tag{2}$$

where V_C and V_O were volume (mL) of the aqueous and oil phases, C_{IN} was the original protein concentration of emulsions (mg/L), C_{SE} was protein concentration in water phase after emulsification (mg/L), and S was the specific surface area of conjugates emulsion (m^2/L).

2.4.1. Determination of bound phenol content of interface protein

The study of Wei et al. (2024) was referenced. The interface proteins

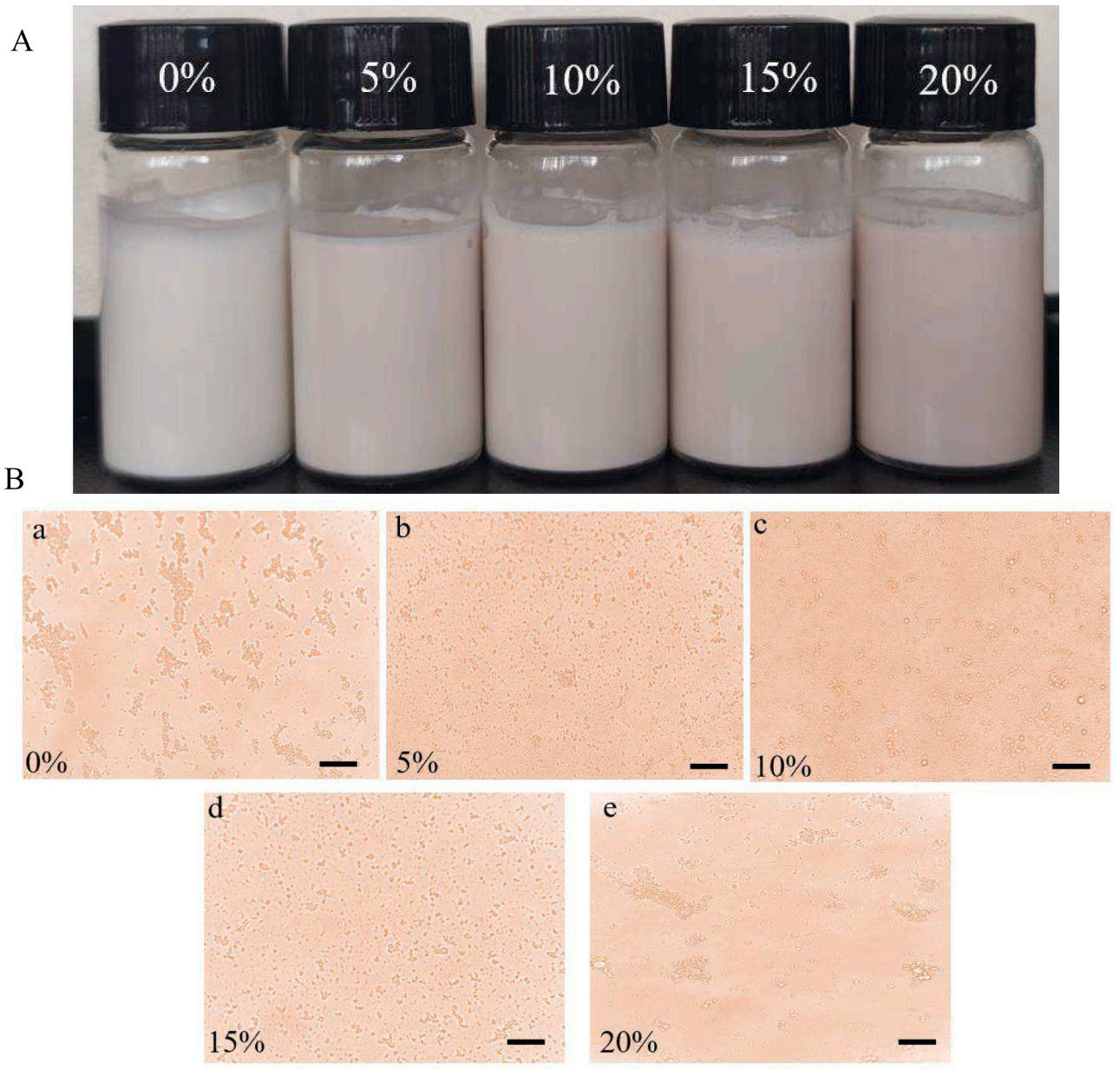

Fig. 1. Effect of EGCG concentration on the appearance (A) and microstructure (B, scale size of 5 μm) of emulsions.

solution (1.0 mg/mL) was precipitated with 5 % trichloroacetic acid and centrifuged. The supernatant was mixed and reacted with the addition of Folin-phenol reagent (1:5, *v*/v) for 5 min, then Na_2CO_3 solution was added, and then the reaction was carried out for 2 h. Finally, the absorbance of the solution was determined at 760 nm. For the determination of total phenol content, the sample solution was blended directly with Folin-phenol reagents. The subsequent method was consistent with that used for the measurement of free phenol content, and bound phenol content was calculated according to the formula (Eq. (3))

$$\text{Bound phenol content } (\mu g/mg) = T_{PC} - F_{PC} \quad (3)$$

where T_{PC} (F_{PC}) indicated total (free) phenol content.

2.5. Structural characterization of IAP and IUAP

2.5.1. Free sulfhydryl and disulfide bonds content

The method of Wei et al. (2024) was referenced. The protein sample was combined with *β*-mercaptoethanol as well as trichloroacetic acid, and centrifuged to collect supernatant. The supernatant was blended with Ellman's reagents to measure absorbance value (412 nm). The content was determined according to the formula (Eq. (4) and Eq. (5)):

$$\text{Total sulfhydryl group } (-SH_T) = 73.53 \times A_{412}/C \quad (4)$$

$$\text{Disulfide bonds } (S\blacksquare S) = (SH_T - SH_R)/2 \quad (5)$$

where 73.53 was molar extinction coefficient; C was the proteins concentrations, SH_R was total sulfhydryl group. SH_T was a free sulfhydryl group.

2.5.2. Sodium dodecyl sulfate polyacrylamide gel electrophoresis (SDS-PAGE)

The approach of Li et al. (2019) was referenced. Briefly, the reduced (containing *β*-mercaptoethanol) and non-reduced SDS-PAGE of protein samples were determined. The loading volume was 10 μL. Electrophoresis was 10 mA at the beginning and 30 mA after the sample entered the

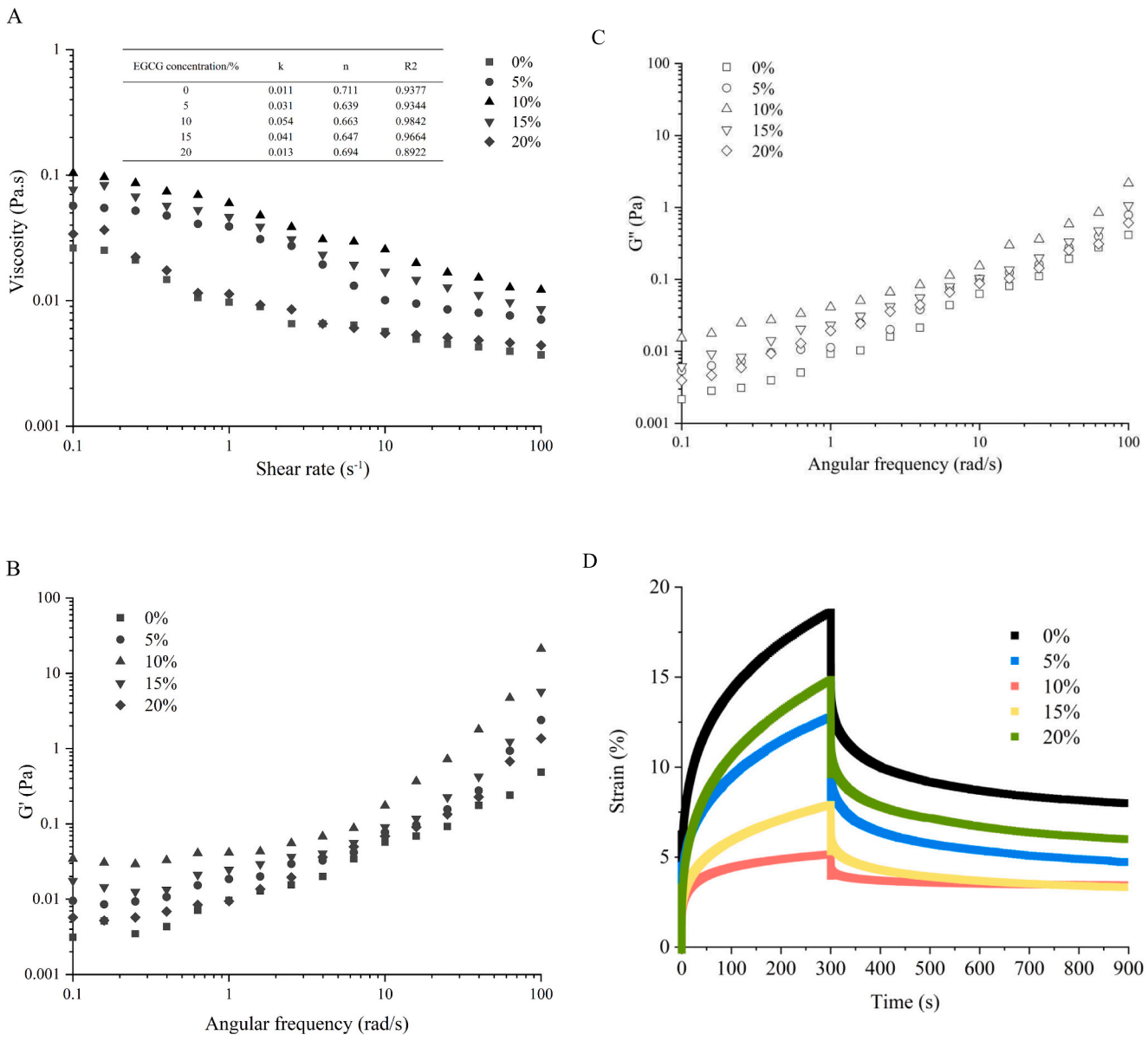

Fig. 2. Effect of EGCG concentration on the rheological properties of emulsions (A: viscosity (the embedded table was fitted with viscosity data), B: G', C: G", D: strain value). Different letters denote significant differences between data ($P < 0.05$).

separating gel.

2.5.3. Average particle size and ζ-potential

The methodology of Zhao et al. (2023) was referenced, with appropriate change. The protein sample was diluted to 1.0 mg/mL using distilled water to measure by a Zetasizer (Malvern Instruments, UK).

2.5.4. Surface hydrophobicity

The method of Zhao et al. (2023) was referenced to determine the surface hydrophobicity of protein. Briefly, different concentrations (0.005–0.5 mg/mL) of protein solution (4 mL) were mixed with ANS (in the dark), and then the fluorescence intensity of the mixed solution was measured by a fluorescence spectrometer (Shimadzu, Kyoto, Japan). The excitation wavelength and emission wavelength were 390 nm and 470 nm, respectively. A slope of fluorescence intensity with the corresponding concentration was the surface hydrophobicity.

2.5.5. Intrinsic fluorescence spectroscopy

The methodology of Li et al. (2019) was referenced, with slightly modification. The excitation wavelength and emission wavelength were 295 nm and 300–480 nm by a fluorescence spectrometer (F-7000, Shimadzu, Japan).

2.5.6. Fourier transform infrared spectra (FT-IR)

The approach of Zhao et al. (2023) was referenced. Simply, the lyophilized conjugates were mixed with dried KBr into thin slices. The samples were scanned for absorbance in the wavenumber range of 4000–400 cm^{-1} by an FT-IR spectrometer (IRTracer-100, Shimadzu Co, Japan). The secondary structure fraction was divided in the amide I region to obtain the percentage.

2.5.7. Trypsin sensitivity of IAP and IUAP

The method of Li et al. (2019) was referenced, with appropriate change. The protein solution was blended with trypsin solution (1 mg/mL), and incubated at 38 °C for 5 min. The reaction was stopped by adding trichloroacetic acid. Finally, the absorbance value (A_{280}) was recorded.

2.6. Statistical analysis

All trials were repeated at least thrice. The data was conducted by SPSS 22. A significant difference ($P < 0.05$) was measured using one-way analysis of variance (ANOVA) with Duncan's multiple range tests. The Origin 2019 software (Originlab, USA) was used to draw graphics.

3. Results and discussion

3.1. Effect of EGCG concentration on microstructure and rheological properties of conjugates emulsions

3.1.1. Appearance and microstructure

As observed in Fig. 1A, the conjugates emulsions presented a homogeneous and stable state. As the EGCG concentration increased (0 %–20 %), the color of the emulsions gradually became darker, which indicated that EGCG was covalently bound to RBP-SPI by alkaline pH-shifting. EGCG was oxidized to quinone under an alkaline condition, and quinones reacted with proteins to produce brown color (Keppler et al., 2020). During the preparation of the emulsions, shearing and high-pressure homogenization treatments disrupted the color of the protein solution compared to the color of conjugate solution itself, which resulted in a change color of emulsion. The droplet sizes of the conjugate emulsions initially declined, and subsequently increased with increasing EGCG concentration (Fig. 1 Ba—Be), which was consistent with microstructure of emulsions by fluorescence microscopy in our previous work (Wei et al., 2024). Previously, we also discovered that the average droplet size of conjugates emulsions declined from 890.85 nm (EGCG concentration of 0 %) to 459.90 nm (EGCG concentration of 10 %), and then increased to 776.30 nm (EGCG concentration of 20 %) (Wei et al., 2024). The conjugates emulsions exhibited a homogeneous distribution and the smallest particle size at an EGCG concentration of 10 %. The phenomena indicated that EGCG improved the agglomerated flocculation of the emulsion. Moderate concentration of EGCG (10 %) facilitated the emulsion stability. Whereas, excessive concentration of EGCG (20 %) led to flocculation of conjugates emulsion, which decreased the stability of conjugates emulsion. Alkaline pH-shifting provided sites of action for covalent binding of EGCG to conjugates (Hao et al., 2022; Wei et al., 2024). The highly flexible conjugate was more easily adsorbed at the O/W interface through hydrophobic interactions, which promoted uniform distribution of small-sized droplets (Hao et al., 2022; Yan et al., 2023). Additionally, polyphenols could promote droplets fragmentation or prevent droplets aggregation during shearing. Excessive concentrations of EGCG caused the formation of aggregates at the O/W interface, which resulted in emulsion flocculation and an increase in droplet size (Wei et al., 2024).

3.1.2. Viscosity

As observed in Fig. 2A, the viscosity of conjugates emulsion declined as shear rate increased, which demonstrated that conjugates emulsions showed the property of shear thinning non-Newtonian fluids (Tan et al., 2024). Droplets in the flocculated state were separated under shear stress, leading to fluid rearrangement (Zhao et al., 2024). The viscosity of emulsions initially increased, and subsequently declined with increasing EGCG concentration. As the concentration of EGCG increased, the k-value of emulsions initially increased from 0.011 to 0.054, and subsequently decreased to 0.013 (the embedded table in Fig. 1). The n-value was always less than 1. The phenomenon showed that moderate concentrations of EGCG enhanced the viscosity of the conjugate emulsion. Moderate concentration of EGCG caused the continuous phase in the emulsions to form a mesh, which increased the viscosity of the interfacial film. Additionally, highly flexible protein promoted the flow resistance of the emulsions through hydrophobic/electrostatic interactions, thereby improving the emulsions viscosity (Wang et al., 2022). However, excessive concentration of EGCG led to disordered aggregation of protein at the O/W interface, reducing the conjugates emulsions viscosity.

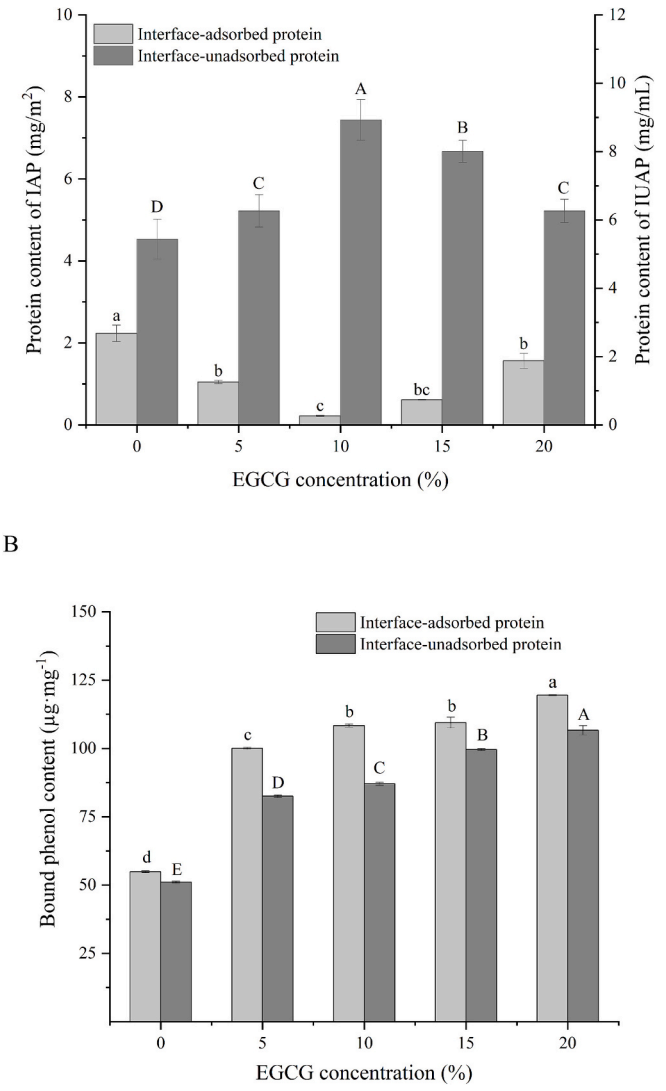

Fig. 3. Effect of EGCG concentration on the protein content (A) and bound phenol content (B) of IAP as well as IUAP (Lowercase letters denote significant differences between IAP, and uppercase letters denote significant differences between IUAP ($P < 0.05$)).

3.1.3. Viscoelasticity

Both G' (Fig. 2B) and G" (Fig. 2C) of the conjugates emulsions initially increased, and subsequently dropped with increasing EGCG concentration. The phenomena suggested that moderate concentration of EGCG enhanced the viscoelasticity of the emulsion, while excessive concentration of EGCG diminished the viscoelasticity of the emulsion (Shen et al., 2023). Moderate concentration of EGCG enhanced flexibility of proteins, and the highly flexible proteins orderly adsorbed at O/W interface through hydrophobic interactions and electrostatic repulsion to form the dense interfacial membrane (Li et al., 2022). In contrast, the accumulation of polyphenols on the hydrophobic side chain of protein impeded protein interfacial rearrangement and the formation of viscoelastic interfacial film (Bock et al., 2022). Excessive concentration of caused polyphenols disordered aggregation of proteins, which weakened the viscoelasticity of the emulsions (Liu et al., 2024).

3.1.4. Creep-recovery

As shown in Fig. 2D, the strain value of the conjugates emulsions initially declined, and then increased with increasing the EGCG

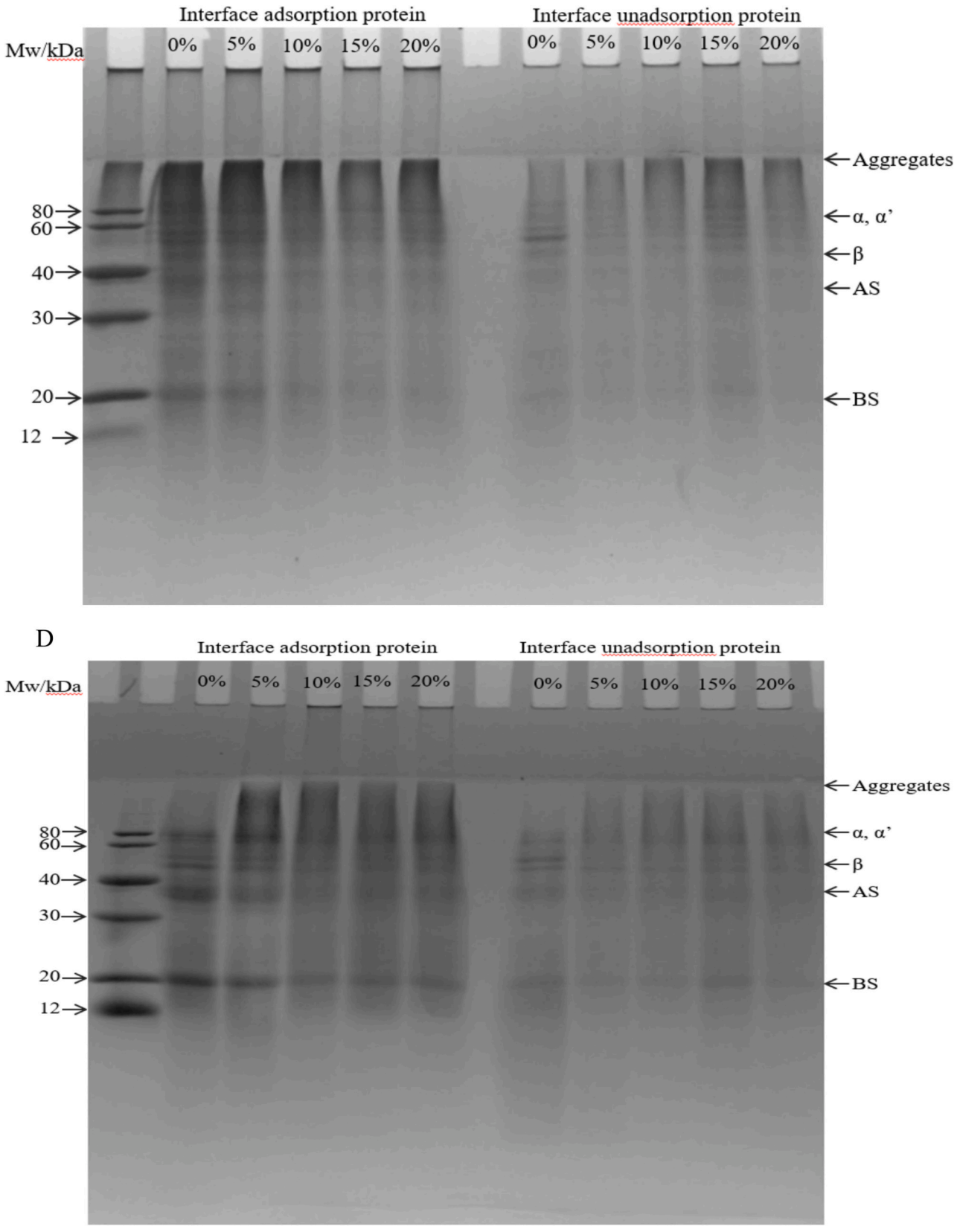

Fig. 4. Effect of EGCG concentration on the free sulfhydryl content (A), disulfide bonds content (B), and SDS-PAGE (C: reduced, D: non-reduced) of IAP and IUAP (Lowercase letters denote significant differences between IAP, and uppercase letters denote significant differences between IUAP ($P < 0.05$)).

concentrations, and reached the minimum value at an EGCG concentration of 10 %. High strain value indicated weaker network structures, small strain indicated stronger network structures (Lu et al., 2019; Wang et al., 2022). Thus, moderate concentration of EGCG could enhance the resistance of emulsion to external stresses by increasing the viscoelasticity of emulsion (Wang et al., 2022; Shen et al., 2023). Excessive concentration of EGCG decreased the strength of emulsions network structure, but it was still stronger than that of RBP-SPI emulsion without EGCG. Excellent viscoelasticity contributed to the strain recovery of emulsions when subjected to external pressures, which was beneficial for food products subjected to a variety of forces during complex applications.

3.2. Effects of EGCG concentration on the structural characteristics of IAP and IUAP

3.2.1. Interface protein content and bound phenol content

As observed in Fig. 3A, the IAP content of conjugates emulsions initially significantly decreased, and subsequently increased as EGCG concentration increased, peaking a minimum value at an EGCG concentration of 10 % ($P < 0.05$). Due to a certain total protein content, the trend of IUAP content showed an opposite trend to the IAP content. Alkaline pH-shifting facilitated unfolding of protein spatial structures, moderate concentration of EGCG bound to RBP-SPI and dispersed in a more ordered condition at O/W interface (Wei et al., 2024). The lower interfacial adsorption content indicated the higher degree of protein unfolding (Drusch et al., 2021). The unfolding of the interfacial protein structure led to a decrease in the oil-water interface film thickness and an increase in protein flexibility, which contributed to the adsorption of proteins at the O/W interface for the formation of viscoelastic interfacial film (Fig. 2B and Fig. 2C) (Tan et al., 2024). Excessive concentration of EGCG adsorbed more protein at the O/W interface, which increased the content of IAP. Excessive adsorption of protein complexes led to squeeze of protein by Coulomb forces, which enhanced the rigidity of the adsorbed layer (Li et al., 2024).

As observed in Fig. 3B, the bound phenol content of interface protein significantly increased ($P < 0.05$) as EGCG concentration increased, which also verified the color change of conjugates emulsions (Fig. 1A). The bound phenol content of IAP was higher than that of IUAP, which indicated that EGCG promoted the distribution of more bound phenols at the interface. The changes in bound phenol content were similar to those found by Tian et al. (2022), who found that tea polyphenols promoted phenol binding to IAP. Alkaline pH-shifting led to the unfolding of proteins structures, which facilitated the binding of moderate concentration of EGCG bound to phenol with interface protein (Wei et al., 2024). Excessive concentration phenols caused polyphenol-protein interactions at the interface to compete with proteins-proteins interactions, thereby disrupting the interfacial films (Bock et al., 2022).

3.2.2. Free sulfhydryl and disulfide bonds content

The free sulfhydryl and disulfide bonds content of both IAP and IUAP (Fig. 4A) significantly decreased as EGCG concentration increased ($P < 0.05$). Disulfide bond and free sulfhydryl content (Fig. 4B) of IUAP were higher than that of IAP. Alkaline pH-shifting led to oxidation of EGCG to form quinones (Wei et al., 2024). The sulfhydryl groups in protein conjugates underwent an addition reaction with a large amount of quinones in the environment, which formed C—S covalent bond and depleted the sulfhydryl groups in the protein (Liu et al., 2024). Additionally, the partial unfolding of the protein spatial structure through alkaline pH-shifting resulted in breakage of disulfide bonds and promoted the formation of C—S covalent bonds between free sulfhydryl and quinone in the environment, which decreased the content of disulfide bonds (Li et al., 2024). IAP partially unfolded at the interface, and its structure was different from that of proteins dissolved in aqueous solution. In contrast to aqueous solutions, the partial unfolding of protein exposed other phenolic compound binding sites, which facilitated

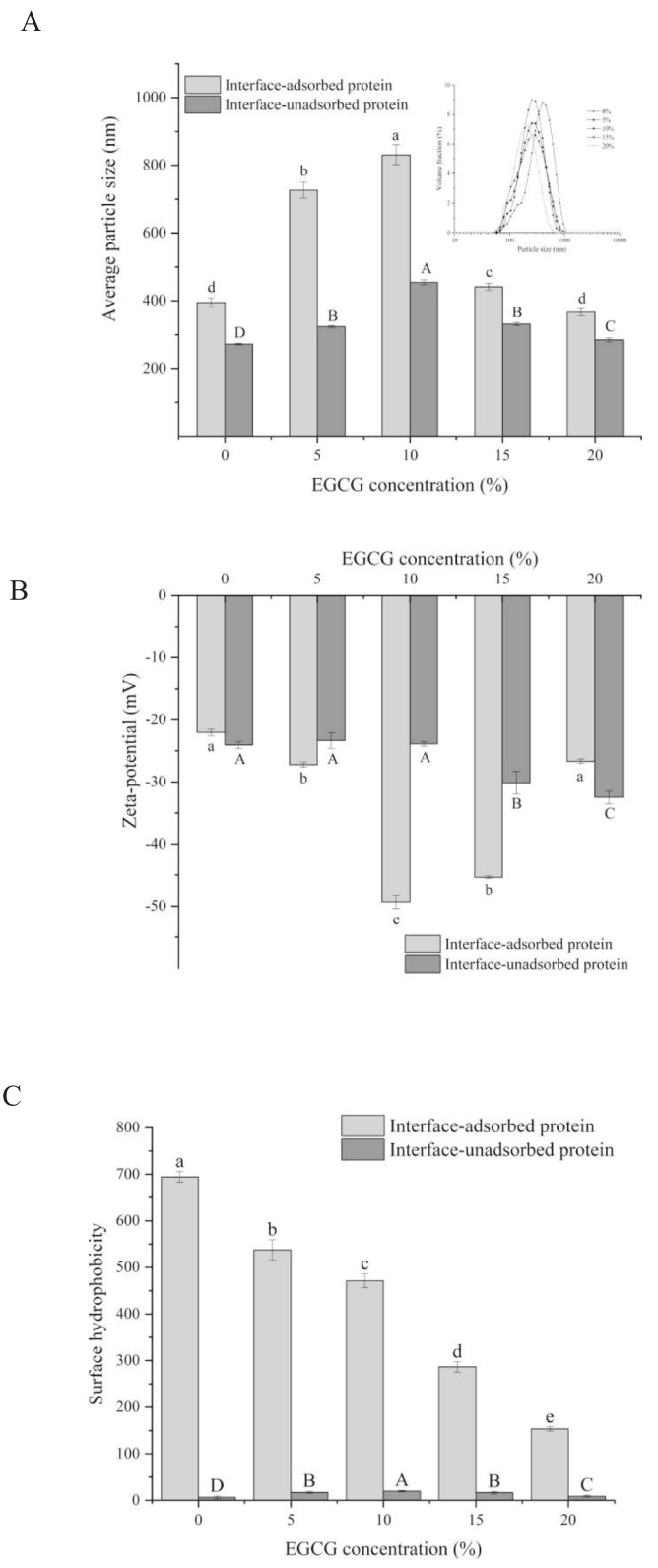

Fig. 5. Effect of EGCG concentration on the particle size (A), ζ-potential (B), and surface hydrophobicity (C) of IAP and IUAP (Lowercase letters denote significant differences between IAP, and uppercase letters denote significant differences between IUAP ($P < 0.05$)).

proteins-phenolic compounds interaction at the interface (Tian et al., 2022). Thus, EGCG had a higher probability of binding to RBP-SPI at the interface, resulting in fewer free sulfhydryl groups and disulfide bonds at the interface for IAP.

3.2.3. SDS-PAGE

As shown in Fig. 4C and Fig. 4D, IAP and IUAP exhibited distinct subunit bands. In reduced SDS-PAGE plot (Fig. 4C), high molecular weight aggregates emerged on the subunit bands of both IAP and IUAP after the addition of EGCG. The intensity of aggregate bands of IAP was stronger than that of IUAP. The phenomena indicated that many non-disulfide covalent bonds existed in the conjugates and majority of which were adsorbed at interface. The phenomenon was similar with the fact that the bound phenol content of IAP was higher than that of IUAP (Fig. 3B). The intensity change of the aggregate bands on IAP was insignificant when the EGCG concentration increased. The presence of much high molecular weight aggregates resulted in aggregates structure that were too large to enter the separating gel (Zhao et al., 2023). In the non-reduced SDS-PAGE plot (Fig. 4D), IAP had high molecular weight aggregates, which did not enter the separating gel. The high molecular weight aggregates were absent from the gel electrophoresis plots of IUAP, implying the presence of more high molecular weight aggregates in IAP. The low molecular weight (40–60 kDa) subunit bands in the IUAP and IAP gradually weakened until they disappeared with an addition of EGCG, demonstrating EGCG interacted with protein.

3.2.4. Particle size and ζ-potential

The average particle size of both IAP and IUAP (Fig. 5A) significantly increased, and subsequently decreased as EGCG concentration increased ($P < 0.05$), reaching the maximum value at an EGCG concentration of 10 %. The moderate concentration of EGCG trended to bind proteins and form stable chain-like protein aggregates, which were uniformly adsorbed at the interface (Li et al., 2024). Excessive EGCG led to the formation of bi-spherical aggregates through dimerization reactions with proteins, leading to reduced particle size (Li et al., 2021).

As observed in Fig. 5B, the interface protein solution (pH 7.0) exhibited a negative charge. The pH of conjugate solution was higher than the isoelectric point of the protein solution. The EGCG also carried a negative charge (Liu et al., 2024). When EGCG concentration increased, the absolute value of ζ-potential of IAP initially significantly increased and subsequently declined, reaching a maximum at an EGCG concentration of 10 % ($P < 0.05$). The unfolding of protein structures exposed the charged amino acids, and moderate concentration of negatively charged EGCG formed electrostatic interactions with positively charged groups on protein molecule (Ke & Li, 2024). The IAP was adsorbed on the surface of emulsions droplet, so absolute value of ζ-potential for IAP determined electrostatic repulsion between emulsion droplet (Li et al., 2022). However, excessive EGCG led to protein aggregation, which partially buried charged amino acids and reduced electrostatic repulsion. Higher electrostatic repulsion contributed to increasing emulsions stability (Zhao et al., 2024). Therefore, moderate concentration of EGCG enhanced the stability of conjugate emulsions.

3.2.5. Surface hydrophobicity

The surface hydrophobicity of IAP was larger than that of IUAP (Fig. 5C), suggesting that the unfolding of proteins spatial structures during adsorption exposed buried hydrophobic groups and promoted proteins rearrangement at the O/W interface (Zhang et al., 2022). The result was consistent with a study by Zhang et al. (2022), who found that conformational changes in protein exposed hydrophobic groups, resulting in more proteins adsorbed at the interface. The exposure of hydrophobic groups facilitated the formation of viscoelastic interfacial film via hydrophobic interactions, thus preventing oil droplets aggregation and stabilizing the emulsion (Chen, Wang, Ma, et al., 2019). The surface hydrophobicity of IAP decreased as EGCG concentration increased ($P < 0.05$). The covalently binding of conjugates to EGCG

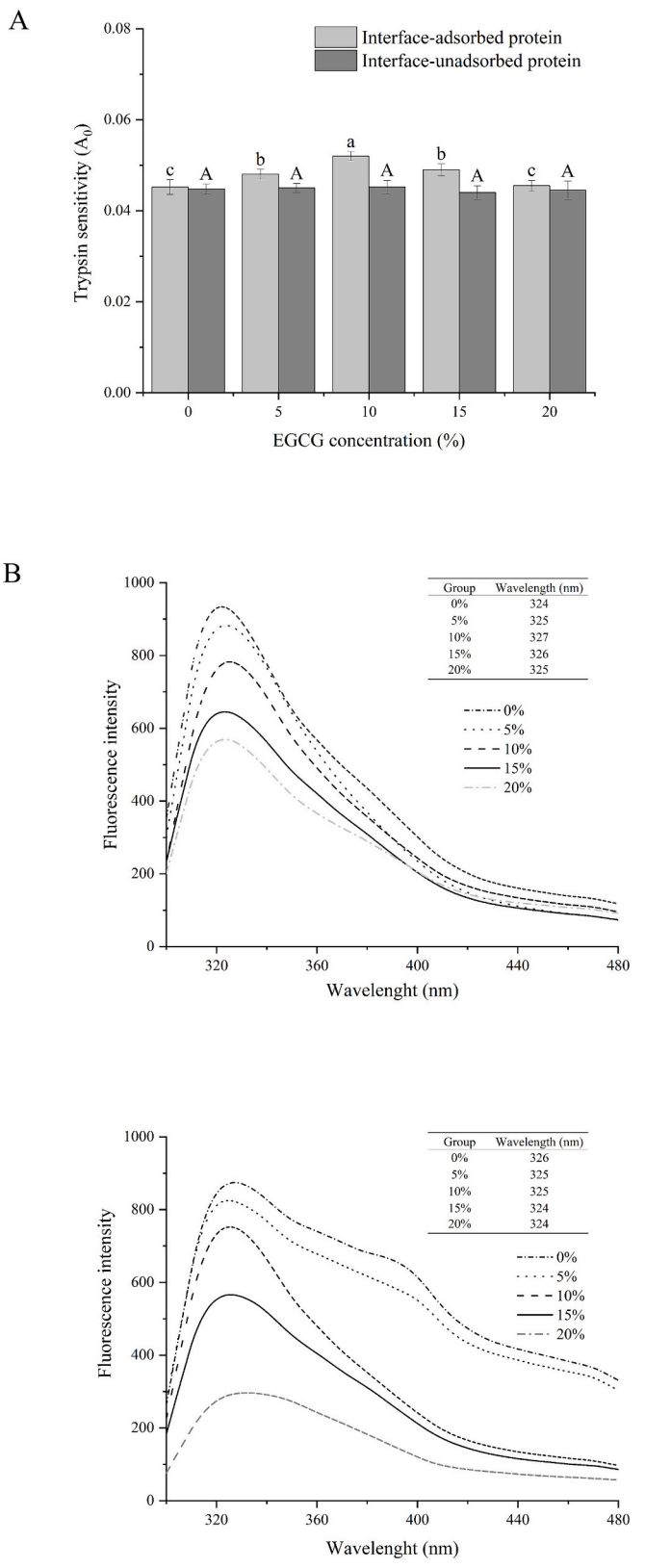

Fig. 6. Effect of EGCG concentration on trypsin sensitivity (A), intrinsic fluorescence of IAP (B) and IUAP (C) (Lowercase letters denote significant differences between IAP, and uppercase letters denote significant differences between IUAP ($P < 0.05$)).

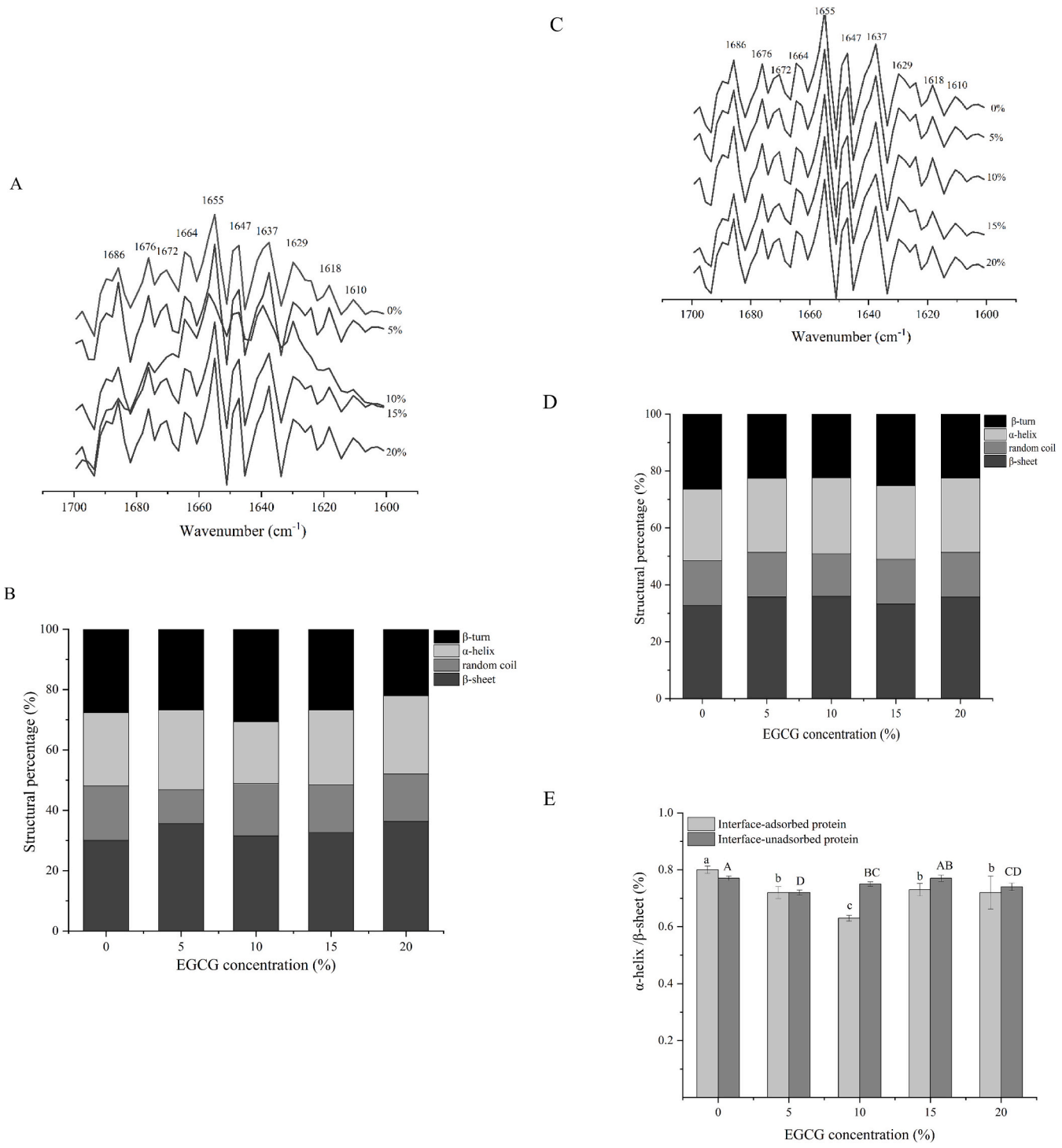

Fig. 7. Effect of EGCG concentration on the secondary structure of IAP and IUAP (A and B were FTIR spectra and secondary structure distributions of IAP; C and D were FTIR spectra and secondary structure distributions of IUAP; E: secondary structural flexibility. (Lowercase letters denote significant differences between IAP, and uppercase letters denote significant differences between IUAP ($P < 0.05$)).

during protein rearrangement by hydrophobic interactions, which reduced the surface hydrophobicity of the interface protein (Lian et al., 2023). In contrast, surface hydrophobicity of IUAP initially increased, and subsequently decreased, reaching the maximum value at an EGCG concentration of 10 % ($P < 0.05$). A moderate concentration of EGCG promoted the adsorption binding of RBP-SPI at the O/W interface, thereby retaining proteins with partially unfolded structure in the aqueous phase (Li et al., 2024). Excessive EGCG inhibited the unfolding of IUAP, thereby reducing the exposure of hydrophobic groups. The hydrophobic interaction between EGCG and protein occurred between the benzene ring on EGCG and the hydrophobic group on the protein. Methionine, leucine, alanine, and lysine residues in RBP/SPI were the sites of hydrophobic interaction (Chen, Wang, Feng, et al., 2019). Therefore, EGCG might interact with methionine, leucine, alanine, and lysine residues to modulate the surface hydrophobicity of interface proteins.

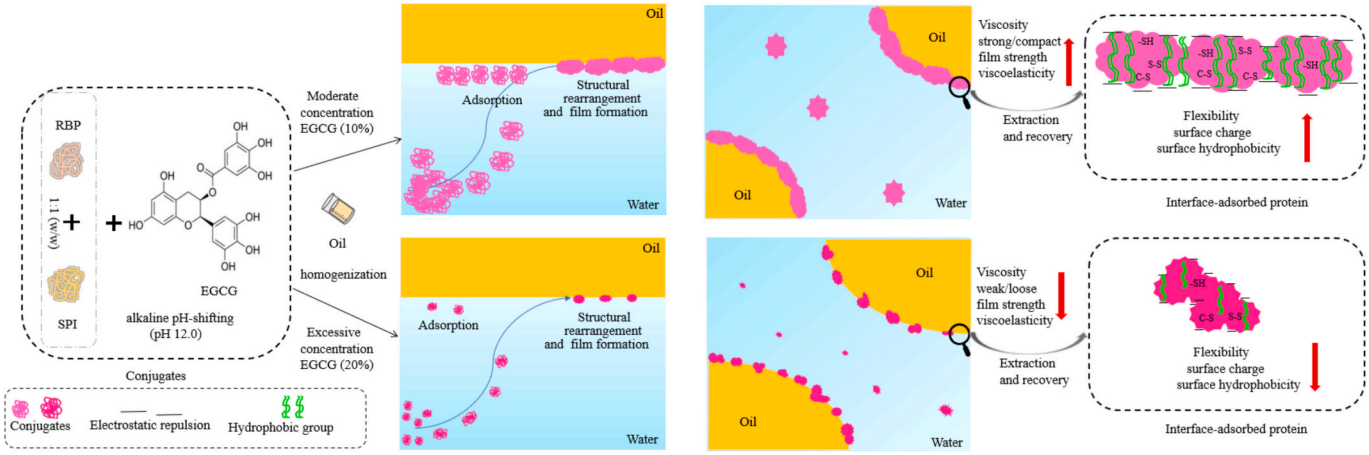

Fig. 8. The schematic diagram of the mechanism by which the structure of interface protein affected the rheological properties of conjugates emulsions.

3.2.6. *Trypsin sensitivity*

The trypsin sensitivity of IAP initially increased, and subsequently declined as EGCG concentration increased, and reached the maximum value at an EGCG concentration of 10 % (Fig. 6A). The phenomena indicated that moderate concentration of EGCG enhanced flexibility of IAP. Whereas, excessive concentration of EGCG decreased the flexibility of IAP. The partial unfolding of protein structure induced by alkaline pH-shifting facilitated the binding of moderate concentration of EGCG to IAP, thereby enhancing the interaction with trypsin (Li et al., 2021). However, excessive concentration of EGCG induced aggregation of protein complexes, which inhibited protein binding to trypsin (Li et al., 2024). The influence of EGCG concentrations on trypsin sensitivity of IUAP was insignificant ($P > 0.05$). The trypsin sensitivity of IAP was higher than that of IUAP. The results suggested that the spatial structure of IAP was more flexible than IUAP. Highly flexible protein was readily adsorbed at the O/W interface to form dense interface films, thus enhancing emulsion viscoelasticity (Wei et al., 2024).

3.2.7. *Intrinsic fluorescence*

As observed in Fig. 6, the fluorescence intensity of IAP progressively declined as EGCG concentration increased, and the maximum emission wavelength initially red-shifted, and subsequently blue-shifted (Fig. 6B). The fluorescence intensity of IUAP slowly decreased, the maximum emission wavelength slowly blue-shifted (Fig. 6C). Moderate concentrations of EGCG promoted the exposure of aromatic amino acids (tryptophan residues) during the unfolding of the protein spatial structure, thereby increasing polarity in the environment (Lian et al., 2023; Wu et al., 2024). Excessive EGCG crosslinked with RBP-SPI to form agglomerates, which buried the fluorescence of tryptophan residues and caused the maximum emission wavelength of IAP to blue-shift. However, the degree of agglomeration induced by excessive EGCG concentration remained lower than that observed in RBP-SPI without EGCG. When EGCG concentration was 10 %, the maximum absorption wavelength of IAP was higher compared to that of IUAP, which suggested unfolding and conformational change in IAP (Lian et al., 2023).

3.2.8. *Secondary structure*

As shown in Fig. 7A and Fig. 7C, there were about 10 major spectral bands of interface proteins in the amide I region. As observed in Fig. 7B and Fig. 7D, the addition of EGCG changed the content of α-helix and β-sheet structure of IAP. These structural variations might be attributed to the formation of hydrogen bonds within the protein molecule (Chen et al., 2024; Dong et al., 2021). Additionally, variations in EGCG concentration had insignificant impact on the secondary structure composition of IUAP, suggesting that the folding and reorganization of conjugates predominantly occurred at the O/W interface. As observed in Fig. 7E, the secondary structure flexibility of IAP initially decreased (with the ratio declining from 0.80 to 0.63), and subsequently increased to 0.72. A lower ratio indicated higher flexibility (Li et al., 2021). The maximum flexibility of IAP was observed at an EGCG concentration of 10 %. Whereas, the IUAP showed insignificant changes in flexibility. This mutual translocation of protein was associated with their differential capacity to undergo the structure alterations during adsorption. Reduced protein adsorption decreased the IAP thickness, resulting in higher flexibility (Wei et al., 2024). The more flexible conjugates readily unfolded at the interface to expose the active group, which further explained the observed changes in the content of bound phenols, sulfhydryl groups, and disulfide bond of IAP.

3.3. *Potential mechanisms by which EGCG affected interface protein conformation and rheological properties of conjugate emulsions*

As shown in the schematic diagram (Fig. 8), the alkaline pH-shifting promoted the binding of EGCG with RBP-SPI to form conjugates. During the adsorption process at the O/W interface, the conjugates underwent structural rearrangement. Moderate concentrations of EGCG promoted the ordered adsorption of highly flexible IAP at the O/W interface through non-covalent interaction (including electrostatic repulsion (Fig. 5B) and hydrophobicity (Fig. 5C) and covalent interaction (involving free sulfhydryl (Fig. 3B), disulfide bonds (Fig. 4A), and C—S bonds). The IAP formed a dense and highly viscoelastic interfacial film at the O/W interface (Fig. 2), and the spatial steric hindrance between droplets prevented aggregation of droplets. EGCG interacted with some amino acid residues (methionine, leucine methionine, alanine methionine, lysine methionine, tryptophan methionine, and aspartic acid residues) in RBP and SPI via hydrophobic interactions and hydrogen bonging, which led to changes in the structural characteristics (particle sizes, ζ-potential, surface hydrophobicity, intrinsic fluorescence, flexibility) of interface proteins (Chen, Wang, Feng, et al., 2019; Xu et al., 2019). Conversely, excessive concentration of EGCG induced the aggregation of interface proteins, which resulted in the burial of hydrophobic and charged groups. This phenomenon weakened the spatial steric hindrance and electrostatic repulsion between emulsion droplets, ultimately resulting in a reduction in the viscosity and viscoelasticity of the emulsions. Therefore, EGCG improved the rheological properties of conjugate emulsions by modulating the conformation of interface protein.

4. Conclusion

The covalent binding of EGCG to RBP-SPI enhanced the rheological properties of the conjugate emulsions by modulating the conformational

characteristics of IAP and IUAP. Especially, the structural changes of IAP were crucial for the rheological properties of emulsions. Moderate concentration of EGCG (10 %) decreased protein content, free sulfhydryl, and surface hydrophobicity of IAP, and increased binding phenol content, particle size, and flexibility of IAP. Correspondingly, moderate concentration of EGCG promoted a more ordered adsorption of IAP at the O/W interface through hydrophobic interactions and electrostatic repulsion, which resulted in the formation of stable and highly viscoelastic interfacial membranes. However, excessive concentration of EGCG (20 %) caused disordered aggregation of protein and reduced the viscoelastic of interfacial film. In the subsequent work, it is necessary to explore the encapsulation performance and delivery potential of RBP-EGCG-SPI conjugated emulsions for lipid-soluble active substances. This study revealed, for the first time, the potential mechanism by which polyphenols affected the rheological properties of mixed vegetable protein emulsions from the perspective of interface protein conformation, and provided guidance for using polyphenols to modulate the stability of protein emulsions.

CRediT authorship contribution statement

Mengmeng Zhao: Writing – review & editing, Writing – original draft, Software, Methodology, Investigation, Formal analysis, Data curation. **Xialing Wei:** Software, Methodology, Formal analysis. **Xiaojuan Wu:** Resources, Project administration, Investigation, Funding acquisition, Conceptualization. **Lizhong Lin:** Software, Resources, Methodology. **Wei Wu:** Writing – review & editing, Resources, Project administration, Investigation, Funding acquisition, Formal analysis, Conceptualization.

Declaration of competing interest

The authors declare that they have no known competing financial interests or personal relationships that could have appeared to influence the work reported in this paper.

Acknowledgments

The work was funded by the Science and Technology Innovation Program of Hunan Province (No. 2024JK2152).

Data availability

Data will be made available on request.

References

Bock, A., Kieserling, H., Rohn, S., Steinhäuser, U., & Drusch, S. (2022). Impact of phenolic acid derivatives on β-lactoglobulin stabilized oil-water-interfaces. *Food Biophysics, 17*(4), 508–522. https://doi.org/10.1007/s11483-022-09737-8

Chen, C., Zhang, S., Cheng, X., Ren, Y., Qian, Y., Zhang, C., et al. (2024). Reducing cherry rain-cracking: Enhanced wetting and barrier properties of chitosan hydrochloride-based coating with dual nanoparticles. *International Journal of Biological Macromolecules, 268*, Article 131660. https://doi.org/10.1016/j.ijbiomac.2024.131660

Chen, G., Wang, S., Feng, B., Jiang, B., & Miao, M. (2019). Interaction between soybean protein and tea polyphenols under high pressure. *Food Chemistry, 277*, 632–638. https://doi.org/10.1016/j.foodchem.2018.11.024

Chen, W., Wang, W., Ma, X., Lv, R., Watharkar, R., Ding, T., et al. (2019). Effect of pH-shifting treatment on structural and functional properties of whey protein isolate and its interaction with (−)-epigallocatechin-3-gallate. *Food Chemistry, 274*, 234–241. https://doi.org/10.1016/j.foodchem.2018.08.106

Dong, Y., Lan, T., Huang, G., Jiang, L., Zhang, Y., & Sui, X. (2021). Development and characterization of nanoparticles formed by soy peptide aggregate and epigallocatechin-3-gallate as an emulsion stabilizer. *LWT- Food Science and Technology, 152*, Article 112385. https://doi.org/10.1016/j.lwt.2021.112385

Drusch, S., Klost, M., & Kieserling, H. (2021). Current knowledge on the interfacial behaviour limits our understanding of plant protein functionality in emulsions. *Current Opinion in Colloid & Interface Science, 56*, Article 101503. https://doi.org/10.1016/j.cocis.2021.101503

Grasberger, K., Hammershøj, M., & Corredig, M. (2023). Stability and viscoelastic properties of mixed lupin-whey protein at oil-water interfaces depend on mixing sequence. *Food Hydrocolloids, 138*, Article 108485. https://doi.org/10.1016/j.foodhyd.2023.108485

Hao, L., Sun, J., Pei, M., Zhang, G., Li, C., Li, C., et al. (2022). Impact of non-covalent bound polyphenols on conformational, functional properties and in vitro digestibility of pea protein. *Food Chemistry, 383*, Article 132623. https://doi.org/10.1016/j.foodchem.2022.132623

Hei, X., Li, S., Liu, Z., Wu, C., Ma, X., Jiao, B., et al. (2024). Characteristics of Pickering emulsions stabilized by microgel particles of five different plant proteins and their application. *Food Chemistry, 139187*. https://doi.org/10.1016/j.foodchem.2024.139187

Hinderink, E., Münch, K., Sagis, L., Schroën, K., & Berton-Carabin, C. (2019). Synergistic stabilization of emulsions by blends of dairy and soluble pea proteins: Contribution of the interfacial composition. *Food Hydrocolloids, 97*, Article 105206. https://doi.org/10.1016/j.foodhyd.2019.105206

Ke, C., & Li, L. (2024). Modification mechanism of soybean protein isolate-soluble soy polysaccharide complex by EGCG through covalent and non-covalent interaction: Structural, interfacial, and functional properties. *Food Chemistry, 448*, Article 139033. https://doi.org/10.1016/j.foodchem.2024.139033

Keppler, J., Schwarz, K., & van der Goot, A. (2020). Covalent modification of food proteins by plant-based ingredients (polyphenols and organosulphur compounds): A commonplace reaction with novel utilization potential. *Trends in Food Science & Technology, 101*, 38–49. https://doi.org/10.1016/j.tifs.2020.04.023

Kieserling, H., Pankow, A., Keppler, J., Wagemans, A., & Drusch, S. (2021). Conformational state and charge determine the interfacial film formation and film stability of β-lactoglobulin. *Food Hydrocolloids, 114*, Article 106561. https://doi.org/10.1016/j.foodhyd.2020.106561

Kim, W., Wang, Y., & Selomulya, C. (2020). Dairy and plant proteins as natural food emulsifiers. *Trends in Food Science and Technology, 105*, 261–272. https://doi.org/10.1016/j.tifs.2020.09.012

Kristensen, H., Denon, Q., Tavernier, I., Gregersen, S., Hammershøj, M., Van der Meeren, P., et al. (2021). Improved food functional properties of pea protein isolate in blends and co-precipitates with whey protein isolate. *Food Hydrocolloids, 113*, Article 106556. https://doi.org/10.1016/j.foodhyd.2020.106556

Li, H., Cai, Y., Li, F., Zhang, B., Wu, X., & Wu, W. (2022). Rancidity-induced protein oxidation affects the interfacial dynamic properties and the emulsion rheological behavior of rice bran protein. *Food Hydrocolloids, 131*, Article 107794. https://doi.org/10.1016/j.foodhyd.2022.107794

Li, H., Li, F., Wu, X., & Wu, W. (2021). Effect of rice bran rancidity on the emulsion stability of rice bran protein and structural characteristics of interface protein. *Food Hydrocolloids, 121*, Article 107006. https://doi.org/10.1016/j.foodhyd.2021.107006

Li, R., True, A., Sha, L., & Xiong, Y. (2024). Structural modification of oat protein by thermosonication combined with high pressure for O/W emulsion and model salad dressing production. *International Journal of Biological Macromolecules, 255*, Article 128109. https://doi.org/10.1016/j.ijbiomac.2023.128109

Lian, Z., Yang, S., Cheng, L., Liao, P., Dai, S., Tong, X., et al. (2023). Emulsifying properties and oil-water interface properties of succinylated soy protein isolate: Affected by conformational flexibility of the interfacial protein. *Food Hydrocolloids, 136*, Article 108224. https://doi.org/10.1016/j.foodhyd.2022.108224

Liu, Y., Li, H., Wei, X., Zhou, X., Wu, W., & Wu, X. (2024). Effect of ultrasonic pretreatment on the structure and emulsion stability of epigallocatechin-3-gallate and rice bran protein complex. *LWT- Food Science and Technology, 199*, Article 116107. https://doi.org/10.1016/j.lwt.2024.116107

Lu, J., Xu, X., & Zhao, X. (2022). Interfacial rheology of alkali pH-shifted myofibrillar protein at O/W interface and impact of tween 20 displacement. *Food Hydrocolloids, 124*, Article 107275. https://doi.org/10.1016/j.foodhyd.2021.107275

Lu, Y., Qian, X., Xie, W., Zhang, W., Huang, J., & Wu, D. (2019). Rheology of the sesame oil-in-water emulsions stabilized by cellulose nanofibers. *Food Hydrocolloids, 94*, 114–127. https://doi.org/10.1016/j.foodhyd.2019.03.001

Shao, J., Yang, J., Jin, W., Huang, F., Xiao, J., Chen, Y., et al. (2024). Regulation of interfacial mechanics of soy protein via co-extraction with flaxseed protein for efficient fabrication of foams and emulsions. *Food Research International, 175*, Article 113673. https://doi.org/10.1016/j.foodres.2023.113673

Shen, Q., Li, J., Shen, X., Zhu, X., Dai, J., Tang, C., et al. (2023). Linear and nonlinear interface rheological behaviors and structural properties of pea protein (vicilin, legumin, albumin). *Food Hydrocolloids, 139*, Article 108500. https://doi.org/10.1016/j.foodhyd.2023.108500

Tan, H., Wu, X., Zhao, M., Li, H., & Wu, W. (2024). Formation of self-assembled fibril aggregates of trypsin-controllably hydrolyzed soy protein and its regulation on stability of high internal phase Pickering emulsions. *Food Chemistry, 140996*. https://doi.org/10.1016/j.foodchem.2024.140996

Tian, L., Zhang, S., Yi, J., Zhu, Z., Cui, L., Decker, E., et al. (2022). Antioxidant and prooxidant activities of tea polyphenols in oil-in-water emulsions depend on the level used and the location of proteins. *Food Chemistry, 375*, Article 131672. https://doi.org/10.1016/j.foodchem.2021.131672

Tian, Y., Sun, F., Wang, Z., Yuan, C., Wang, Z., Guo, Z., et al. (2023). Research progress on plant-based protein Pickering particles: Stabilization mechanisms, preparation methods, and application prospects in the food industry. *Food Chemistry: X, 101066*. https://doi.org/10.1016/j.fochx.2023.101066

Wang, Y., Yang, J., Dai, S., Tong, X., Tian, T., Liang, C., & Li, L. (2022). Formation of soybean protein isolate-hawthorn flavonoids non-covalent complexes: Linking the physicochemical properties and emulsifying properties. *Ultrasonics Sonochemistry, 84*, Article 105961. https://doi.org/10.1016/j.ultsonch.2022.105961

Wei, X., Li, H., Liu, Y., Lin, Q., Wu, X., & Wu, W. (2024). Effect of epigallocatechin-3-gallate modification on the structure and emulsion stability of rice bran protein in the presence of soybean protein isolate. *International Journal of Biological*

Macromolecules, 263, Article 130269. https://doi.org/10.1016/j.ijbiomac.2024.130269

Wu, Y., Wu, Y., Xiang, H., Chen, S., Zhao, Y., Cai, Q., et al. (2024). Emulsification properties and oil-water interface properties of l-lysine-assisted ultrasonic treatment in sea bass myofibrillar proteins: Influenced by the conformation of interfacial proteins. *Food Hydrocolloids, 147*, Article 109405. https://doi.org/10.1016/j.foodhyd.2023.109405

Xu, J., Hao, M., Sun, Q., & Tang, L. (2019). Comparative studies of interaction of β-lactoglobulin with three polyphenols. *International Journal of Biological Macromolecules, 136*, 804–812. https://doi.org/10.1016/j.ijbiomac.2019.06.053

Yan, X., Zeng, Z., McClements, D., Gong, X., Yu, P., Xia, J., et al. (2023). A review of the structure, function, and application of plant-based protein-phenolic conjugates and complexes. *Comprehensive Reviews in Food Science and Food Safety, 22*(2), 1312–1336. https://doi.org/10.1111/1541-4337.13112

Zhang, W., Lu, J., Zhao, X., & Xu, X. (2022). An optimized approach to recovering O/W interfacial myofibrillar protein: Emphasizing on interface-induced structural changes. *Food Hydrocolloids, 124*, Article 107194. https://doi.org/10.1016/j.foodhyd.2021.107194

Zhao, M., Li, F., Li, H., Lin, Q., Zhou, X., Wu, X., et al. (2024). Effects of rice bran rancidity on the interfacial adsorption properties of rice bran protein fibril aggregates and stability of high internal phase Pickering emulsions. *Food Chemistry, 443*, Article 138611. https://doi.org/10.1016/j.foodchem.2024.138611

Zhao, M., Wu, X., Li, F., Li, H., & Wu, W. (2023). Effect of rice bran rancidity on the structural characteristics and rheological properties of rice bran protein fibril aggregates. *Food Hydrocolloids, 144*, Article 108959. https://doi.org/10.1016/j.foodhyd.2023.108959

Zolqadri, R., Damani, M., Malekjani, N., Kharazmi, M., & Jafari, S. (2023). Rice bran protein-based delivery systems as green carriers for bioactive compounds. *Food Chemistry, 136121*. https://doi.org/10.1016/j.foodchem.2023, 136121